



**HAL**  
open science

# Design and optimization of industrial woody biomass pretreatment addressed by a multiscale computational model: particle, bed and dryer levels

Julien Colin, Romain Remond, Patrick Perre

## ► To cite this version:

Julien Colin, Romain Remond, Patrick Perre. Design and optimization of industrial woody biomass pretreatment addressed by a multiscale computational model: particle, bed and dryer levels. 19th International Drying Symposium IDS'2014, Aug 2014, Lyon, France. hal-01824101

**HAL Id: hal-01824101**

**<https://hal.science/hal-01824101>**

Submitted on 26 Jun 2018

**HAL** is a multi-disciplinary open access archive for the deposit and dissemination of scientific research documents, whether they are published or not. The documents may come from teaching and research institutions in France or abroad, or from public or private research centers.

L'archive ouverte pluridisciplinaire **HAL**, est destinée au dépôt et à la diffusion de documents scientifiques de niveau recherche, publiés ou non, émanant des établissements d'enseignement et de recherche français ou étrangers, des laboratoires publics ou privés.

## DESIGN AND OPTIMIZATION OF INDUSTRIAL WOODY BIOMASS PRETREATMENT ADDRESSED BY A MULTISCALE COMPUTATIONAL MODEL: PARTICLE, BED AND DRYER LEVELS

J. Colin<sup>1</sup>, R. Rémond<sup>2</sup>, P. Perré<sup>3\*</sup>

<sup>1</sup>Ministère de l'Agriculture, de l'Agroalimentaire et de la Forêt  
3, rue Babet de Jouy, Paris, 75349 07 SP, France

<sup>2</sup>Université de Lorraine, LERMAB, ENSTIB  
27, rue Philippe Séguin, Épinal, 88026, France

<sup>3</sup>École Centrale Paris, LGPM  
Grande Voie des Vignes, Châtenay-Malabry, 92295, France

\*Corresponding author: Tel.: +33 1 41 13 16 79, E-mail: patrick.perre@ecp.fr

**Abstract:** The thermochemical conversion processes of biomass to energy are more and more demanding in the quality of the raw material, especially regarding its moisture content. The use of continuous dryers is tempting because of their low cost and perfect integration in the production line. However the design of the drying chamber and of the heating source and the maximization of the material flow are tedious. With the help of two case studies, this paper aims at proving the potential of a multiscale computational model – considering particle, bed and dryer levels – to design and optimize industrial plants used for wood pretreatment.

**Keywords:** biomass pretreatment, wood energy, continuous dryers, multiscale modelling, design and optimization

### INTRODUCTION

The bioeconomy – *i.e.* the use of biomass for food, feed, industrial and energy purposes<sup>[1]</sup> – is one of the relevant responses to the climate change, to the increasing cost of hydrocarbon and to the energy dependence of France. In this context, the thermochemical conversion processes are promising for a wide range of applications such as heat, biomolecules or biofuels.<sup>[2]</sup> These dry conversion routes require more and more improvement in the quality of raw material, particularly regarding its moisture content (*MC*). The use of continuous dryers for pretreatment of wood energy is then tempting because of their low operating cost and their perfect integration in the production line.

However it is not without pitfall: the climatic conditions heterogeneity inside the dryer together with the biomass variability make the conception and optimization of these industrial plants tedious. Identifying the best technical solutions and estimating their gains through empirical knowledge may be costly in time and money. At first glance, simulation models seem therefore to be the ideal tools, either for the optimal design or for on-line

control. However, the various spatial scales involved in such processes together with the huge variability of biomass render this modeling goal quite challenging.

At the dryer scale, the air parameters change along the flow. This profile of climatic conditions depends on the heat and mass transfers at the exchange surfaces – wood particles and wall of the dryer – and vice versa: the relative humidity (*RH*) and temperature of the air affect the drying rate of each particle. Therefore the two-way coupling between two spatial scales (particle ↔ dryer) is mandatory to simulate the continuous drying of a bed of wood particles.<sup>[3,4]</sup> Some numerical approaches use the concept of distributed micro-models. It allows the two-way coupling to be comprehensive even when all particles are different. Thus it is possible to assess the dryer efficiency regarding its ability to lower the heterogeneity of final *MC* of particles, in spite of the initial variability.

Inside the particle, Finite Element or Control Volume based computational models are very efficient in predicting the evolution of the variable fields (temperature, *MC*, pressure, strain, stress) in the biomass particle. They are also well adapted to deal

with non-linearities and couplings or to test various formulations or parameter values. In this sense, they are able of predictive simulations and can also assist the improvement of the fundamental understanding.<sup>[5,6,7,8]</sup> As drawbacks, they usually lead to significant computation times, which limits the total number of particles at the drier scale. In addition, particular phenomena such as the effect of checks on transfer are difficult to consider. That is why analytical models<sup>[9,10,11]</sup> are often employed to simulate the drying of a large number of particles as it is the case for the pretreatment of biomass. The concept of characteristic drying curve defines the drying rate as a proportion of the maximum drying rate, obtained during the so-called first drying period, when the exchange surface still contains free water. This proportion is a dimensionless function of  $MC$ . However, a usual assumption in the approach proposed by Van Meel<sup>[11]</sup> is that all the energy supplied to the sample is used to evaporate the water. This coarse assumption leads to a poor agreement between simulations and experimental results during certain drying periods, namely during transient periods such as heating-up.<sup>[9,12]</sup> Without considering the sensible heat, models cannot faithfully simulate the evolution of the wood  $MC$  if the airflow temperature varies – as we can notice it along the tunnel of drying – and predict the phenomena of condensation or heating-up.

This paper aims at proving the potential of a multiscale computational model to design and optimize industrial plants used for wood energy pretreatment. Physical formulation of this model at the particle and the dryer scale is presented in the following part. Then the relevance of the multiscale model as an operational tool will be illustrated with the help of two case studies: the optimization of a fix-bed dryer and the design of a conveyor dryer.

## AN INTERACTIVE, FLEXIBLE AND REALISTIC MULTISCALE MODEL

*At the particle scale: an enhanced Van Meel model*

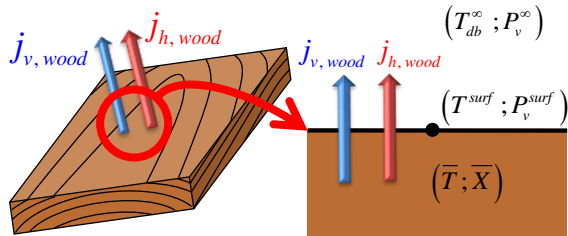


Fig. 1. Heat and mass fluxes at the surface of the particle

The *local* model intends to predict the evolution of the parameters of a wood particle ( $MC$  and temperature) as a function of the surrounding climatic conditions (Fig. 1).

At this scale, we proposed an enhanced Van Meel model, able to account for the coupling between heat and mass transfers in an explicit way<sup>[13]</sup>:

$$\begin{aligned} j_{v,wood} \cdot A_{wood} &= -\dot{\bar{X}} \cdot m_0 \\ &= k_m \cdot C \cdot M_v \cdot A_{wood} \cdot \ln \frac{P_{atm} - P_v^\infty}{P_{atm} - P_v^{surf}} \end{aligned} \quad (1)$$

$$\begin{aligned} j_{h,wood} \cdot A_{wood} &= -h \cdot (T_{db}^\infty - \bar{T}) \cdot A_{wood} \\ &= -m_0 \cdot (c_{p,wood} + \bar{X} \cdot c_{p,l}) \cdot \dot{\bar{T}} + m_0 \cdot L_v(\bar{T}) \cdot \dot{\bar{X}} \end{aligned} \quad (2)$$

In these equations,  $m_0$  is the dry mass of the particle;  $C$  is the molar concentration in the boundary layer and  $A_{part}$  is the area of the particle exchange surface. The main assumption of this model is that the temperature of the studied particles is uniform inside the particle.

The vapor pressure at the surface of the particle is evaluated through the water activity  $a$ :

$$P_v^{surf} = a(\phi, RH) \cdot P_{vs}(\bar{T}) \quad (3)$$

During drying, the value of  $a$  decreases from 1, when free water exists at surface, to  $RH$ , when the particle is in equilibrium with the surrounding air. Following the concept of characteristic drying curve, the water activity is a function of  $RH$  and  $\phi$ , the dimensionless  $MC$  of wood:

$$\phi = \begin{cases} 1 & \text{if } \bar{X} \geq X_{cr} \\ \frac{\bar{X} - X_{eq}}{X_{cr} - X_{eq}} & \text{if } \bar{X} < X_{cr} \end{cases} \quad (4)$$

In order to faithfully simulate the evolution of the particle parameters,  $a$  must be previously identified from drying kinetics of single particles under different levels of temperature and  $RH$ . The function  $a$  can be identified from experimental results for any geometry or any tree species. The 3D version of *TransPore*<sup>[14]</sup>, a computational model simulating the heat and mass transfers in porous media, can also be used to generate drying curves for a wide range of climatic conditions and for any particle size. Note however that *TransPore* is currently validated only for beech and spruce.

Equations (1) and (2) are discretized in time using the Taylor series formulation, truncated at the first order, via a fully explicit scheme. The state of the system and the flux are supposed to be constant between times  $t$  and  $t+\Delta t$ .

*From the particle to the dryer: a multiscale approach*

The *global* model calculates the evolution of the air and wood parameters along the drying chamber, using all fluxes exchanged between each particle. The system of equations describing the *stack*

configuration<sup>[4]</sup> takes into account the two-way coupling between the particle and dryer scales<sup>[13]</sup>:

$$\frac{\partial q_{m,v}}{\partial x} = j_{v,wood} \cdot A_{lin,spe.,wood} + j_{v,wall} \cdot A_{lin,spe.,wall} \quad (5)$$

$$\begin{aligned} & (q_{m,a} \cdot c_{P,a} + q_{m,v} \cdot c_{P,v}) \cdot \frac{\partial T_{db}^{\infty,in}}{\partial x} \\ & = A_{lin,spe.,wood} \cdot (j_{h,wood} + j_{v,wood} \cdot c_{P,v} \cdot (T_{wood} - T_{db}^{\infty,in})) (6) \\ & + A_{lin,spe.,wall} \cdot (j_{h,wall} + j_{v,wall} \cdot c_{P,v} \cdot (T_{wall} - T_{db}^{\infty,in})) \end{aligned}$$

$A_{lin,spe.}$  refers to a linear specific area – in square meter of exchange surface wood/air or wall/air per linear meter of kiln along its main axis *i.e.* the direction of biomass displacement.

In this model, it is assumed that the climatic conditions are homogeneous in the dryer cross-section.

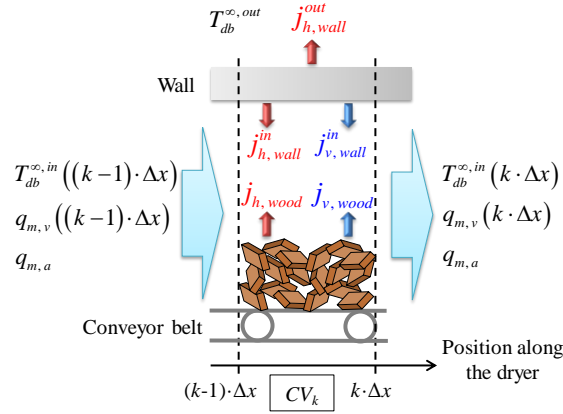


Fig. 2. Heat and mass fluxes inside a Control Volume for a conveyor dryer

Equations (5) and (6) are discretized in space by using the Taylor series formulation, truncated at the first order, via a fully explicit scheme. The dryer is then split along its main axis into  $N$  Control Volumes (CV), each containing  $M$  particles (Fig. 2). For the  $k^{\text{th}}$  CV, the state of the system and the flux are supposed to be constant between the positions  $(k-1) \cdot \Delta x$  and  $k \cdot \Delta x$ .

The climatic conditions along the dryer are evaluated from local heat and mass fluxes simulated for each particle. Thus, the *global* model is connected to thousands of *local* models (enhanced Van Meel model) which confirms the relevance of having a computing time as low as possible for each particle. In order to improve its predictive potential, the *global* model takes into account the heat losses and the possible condensation at the kiln wall.

The computational solution of the multiscale model is encoded in a custom software, written in *Fortran 90*.

Particular attention is paid to the structure of the model so that it is suitable for a wide range of continuous dryers: it can handle parallel- and counter-flow configurations, several air injection or exhaust points and air recirculation.

This new multiscale model is then validated by comparing simulations and experimental kinetics collected thanks to an original device.<sup>[13]</sup>

With the help of two – fictitious but relevant – case studies, the following sections aim at proving the potential of this multiscale computational model as an engineering tool.

## OPTIMIZATION OF A FIXED BED DRYER

### Description of the studied case

A company needs to produce one ton per hour (anhydrous mass flow-rate) of dry wood with an average *MC* less than 20 % and an heterogeneity of *MC* lower than 10 %.

After harvesting, woody biomass is ground into large wood chips ( $60 \times 40 \times 20$  mm). The macroporosity of the granular medium is equal to 0.6. It is then stored in bulk to let it dry in open air for a few weeks, down to an average *MC* of 60% with a standard deviation of 5%. Finally the drying is finished in an industrial plant (Fig. 3). The wood goes through a vertical drying tower from top to bottom and the air from bottom to top: this is a counter-flow configuration. The dryer is supplied with warm air through a waste heat source from nearby industrial facility. The inlet temperature of the air is 60 °C, its *RH* is 4.3 % and its volume flow-rate is  $5 \text{ m}^3 \cdot \text{s}^{-1}$ . The values of heat and mass transfer coefficient are respectively equal to  $49 \text{ W} \cdot \text{m}^{-2} \cdot \text{K}^{-1}$  and  $0.046 \text{ m} \cdot \text{s}^{-1}$ .

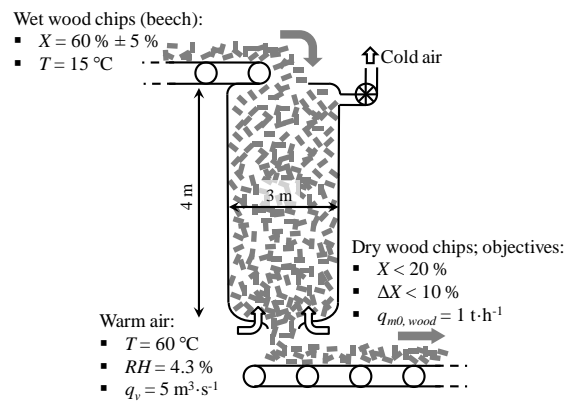


Fig. 3. Schematic description of the fixed bed dryer

The wall is composed with a single steel sheet thermally insulated by a layer of glass wool covering its outer face (Table 1).

Table 1. Characteristics of the drying tower wall

	thickness cm	$\rho$ $\text{kg}\cdot\text{m}^{-3}$	$c_p$ $\text{J}\cdot\text{kg}^{-1}\cdot\text{K}^{-1}$	$\lambda$ $\text{W}\cdot\text{m}^{-1}\cdot\text{K}^{-1}$
steel	1	7500	450	45
glass wool	11	1039	35	0.039
equivalent	12	$\rho\cdot c_p$ ( $\text{J}\cdot\text{m}^{-3}\cdot\text{K}^{-1}$ ) $314\cdot 10^3$		0.043

The external climatic conditions are constant: air temperature is 15 °C, *RH* is 50 % and the value of heat transfer coefficient is  $8 \text{ W}\cdot\text{m}^{-2}\cdot\text{K}^{-1}$ .

The first trials show that the quality of drying does not meet the specifications. The multiscale model is then used in order to identify the technical obstacles to overcome and choose the technical solutions to implement.

#### The non-optimized configuration

The flow-rate is set in order to meet the quantitative needs in dry wood of the company – one ton per hour.

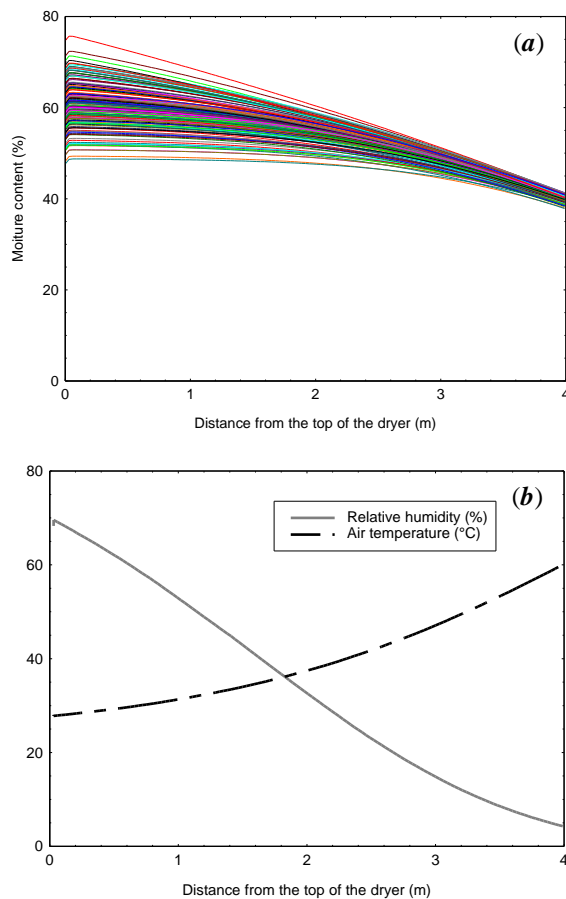


Fig. 4. Simulated evolution of the wood particles *MC* (a) and of the climatic conditions (b) along the dryer for the non-optimized configuration

This configuration does not achieve the qualitative requirements for the downstream processes: out of the dryer, the average *MC* of wood chips is

approximately 40 % (Fig. 4). It is therefore necessary to identify technical solutions to optimize this configuration.

#### Decrease of the wood flow-rate

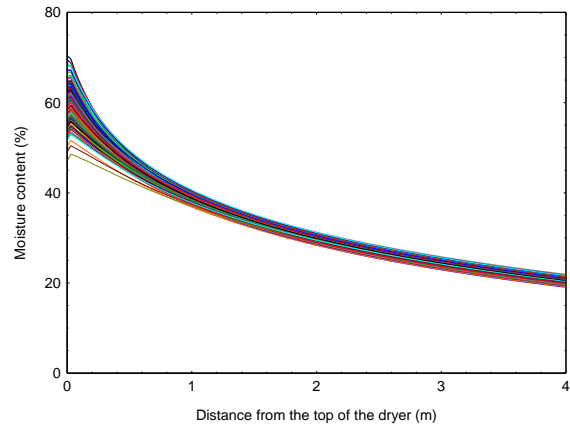


Fig. 5. Simulated evolution of the wood particles *MC* for a bed speed equal to  $0.21 \text{ m}\cdot\text{h}^{-1}$  ( $330 \text{ kg}\cdot\text{h}^{-1}$ )

With a wood flow-rate equal to  $330 \text{ kg}\cdot\text{h}^{-1}$ , the average *MC* of the biomass reaches 20 % at the outlet of the dryer and the dispersion of these values is about 3 % (Fig. 5). This configuration achieves the qualitative objectives. However, from a quantitative point of view, the mass flow-rate of dry wood is just one-third of the company's needs.

#### Reduction of the particle size

The analysis of Fig. 4-b tells us that the air is not fully saturated with moisture at the outlet of the dryer. Thus the evaporation capacity of the fluid is not totally exploited. The resistance to internal transfers within the large wood chips appears to limit the drying rate. In order to test this hypothesis, we study the drying of smaller wood chips:  $20\times 20\times 5 \text{ mm}$ .

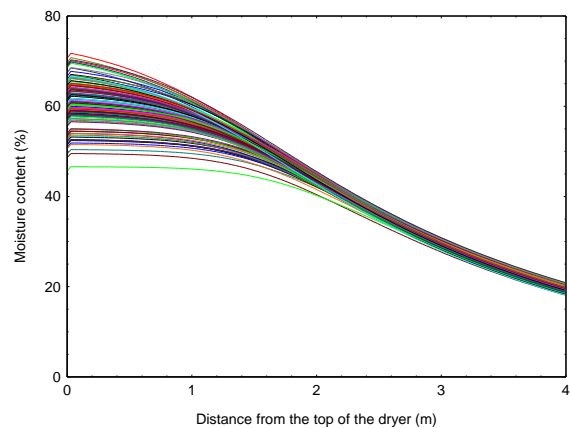


Fig. 6. Simulated evolution of the *MC* of small wood chips for a bed speed equal to  $0.40 \text{ m}\cdot\text{h}^{-1}$  ( $620 \text{ kg}\cdot\text{h}^{-1}$ )

The quality requirements limit the flow-rate of small wood chips to  $620 \text{ kg}\cdot\text{h}^{-1}$  (Fig. 6). Of course it is

lower than the objective flow-rate ( $1 \text{ t}\cdot\text{h}^{-1}$ ) but it is almost twice as high as the maximum flux previously identified for the large particles ( $330 \text{ kg}\cdot\text{h}^{-1}$ ).

Table 2. Summary of qualitative, quantitative and energy aspects of the studied configurations

wood chips	flow-rate ( $\text{kg}\cdot\text{h}^{-1}$ )	outlet MC (%)	outlet air		yield (%)
			T ( $^{\circ}\text{C}$ )	RH (%)	
large	1000	39.9	27.7	67.8	56.8
	330	20.1	41.4	24.6	37.5
small	1000	36.2	23.3	98.8	67.1
	620	20.0	24.9	92.5	70.6

With the initial size of wood chips, the drying rate was indeed controlled by the resistance to internal transfers. It is then not possible to exploit the full evaporation potential of the air (Table 2): at outlet, the air remains warm ( $41.4 \text{ }^{\circ}\text{C}$ ) and far from saturation ( $24.6 \%$ ). Thus it is not surprising that this open system (no air recirculation device) has a very low energy yield ( $37.5 \%$ ). The reduction of the wood chips size is therefore a simple and efficient solution to optimize the drying performance. However, before implementing this solution, the company must ensure that this particle size is compatible with the downstream processes. Furthermore, the additional cost of grinding should be evaluated *ex ante*.

#### Additional heat source

Whatever the particle size, an additional heat source is needed to reach the objective of wood flow-rate ( $1 \text{ t}\cdot\text{h}^{-1}$ ). The multiscale model is then useful to define the required power. Two parameters of the heat source can be adjusted: the flow-rate and its temperature.

For the drying of small wood chips ( $20\times 20\times 5 \text{ mm}$ ), we choose to increase the warm air flow-rate without changing its temperature ( $60 \text{ }^{\circ}\text{C}$ ). This flow-rate must reach  $8.3 \text{ m}^3\cdot\text{s}^{-1}$  – i.e.  $3.3 \text{ m}^3\cdot\text{s}^{-1}$  more than previously – in order to meet all the specifications. The corresponding additional power is  $160 \text{ kW}$ .

If the downstream processes are not compatible with a fine grinding, an increase in the air temperature has two positive effects; a better evaporation potential and a thermal activation of internal transfers, which is very useful for large particles ( $60\times 40\times 20 \text{ mm}$ ). With an air flow-rate equal to  $8.3 \text{ m}^3\cdot\text{s}^{-1}$ , the temperature should reach  $83 \text{ }^{\circ}\text{C}$  to ensure the quality of the dry wood. The additional heating power is then  $327 \text{ kW}$ .

Whether by determining the power of the additional heat source needed or by calculating the energy performance of each configuration, the multiscale model is a powerful tool for the optimization of existing dryers.

## DESIGN OF A CONVEYOR DRYER

### Description of the studied case

A company needs to produce  $450 \text{ kg}\cdot\text{h}^{-1}$  (anhydrous flow-rate) of dry wood for the production of charcoal. Before carbonization, the mean and the heterogeneity of the wood MC must be lower than respectively  $15\%$  and  $10\%$ . The woody biomass is composed of eucalyptus logs (assumed to be cylindrical):

Table 3. Characteristics of eucalyptus logs to dry

parameter	mean	standard deviation
length (mm)	300	20
diameter (mm)	85	5
density ( $\text{kg}\cdot\text{m}^{-3}$ )	600	/
initial MC (%)	90	10
temperature ( $^{\circ}\text{C}$ )	20	/
bed macroporosity	2/3	/

The company wants to build an industrial continuous dryer to pretreat this wet raw material. In order to reduce the operating costs, the dryer will be supplied with warm air through a waste heat source from a nearby industrial facility: the inlet temperature of the air is  $120 \text{ }^{\circ}\text{C}$ , its RH is  $0.59 \%$  and its volume flow-rate is  $4.5 \text{ m}^3\cdot\text{s}^{-1}$ . The use of a conveyor dryer is appropriate due to the large particles size. The conveyor belt carries a  $50 \text{ cm}$  thick bed of logs – a thin bed compared to the particle size – through a tunnel. The cross-section inside this tunnel is  $1 \text{ m}$  high and  $3 \text{ m}$  wide. The wall consists of a  $200 \text{ mm}$  thick inner layer of concrete and a  $100 \text{ mm}$  thick outer layer of glass wool.

By using the multiscale model, we must identify the best airflow configuration. The objective is to meet the specifications while designing a dryer as short as possible in order to reduce the investment costs.

### Simple airflow configurations

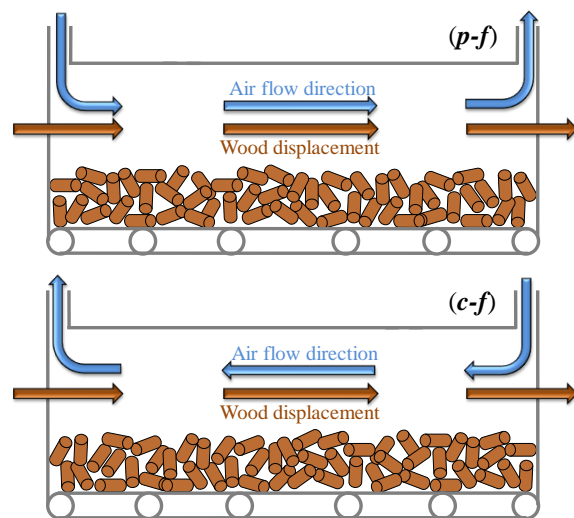


Fig. 7. Simple airflow configurations: parallel-flow, (p-f) and counter-flow (c-f)

In the case of simple configurations, the tunnel has a single point of air injection and a single point of air exhaust (Fig. 7).

Table 4. Qualitative analysis of climatic conditions along the tunnel

position along the tunnel	parameter	<i>p-f</i> config.	<i>c-f</i> config.
beginning	air temperature	high	low
	<i>RH</i>	low	high
	wood temperature	low	low
	condensation at the surface of the particles	no	yes
end	air temperature	low	high
	<i>RH</i>	high	low
	wood temperature	low	high
	equilibrium <i>MC</i>	high	low
<b>length of the tunnel (m)</b>		20.75	<b>10</b>

The *c-f* configuration is the most efficient (Table 4): the tunnel is 10 m long, *i.e.* twice as short as in the case of the *p-f* configuration: 20.75 m.

#### Combined airflow configurations

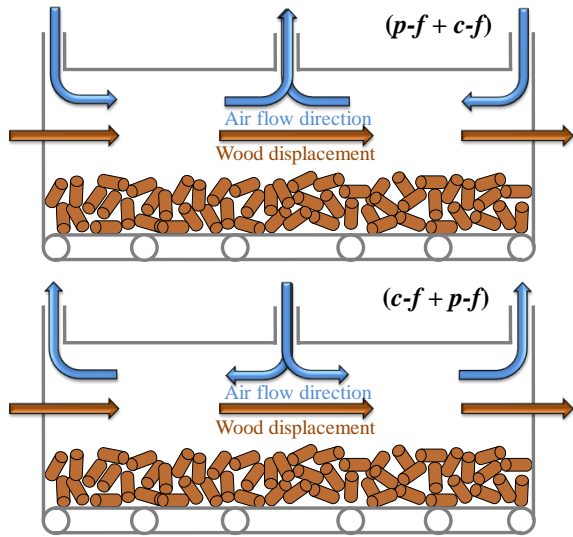


Fig. 8. Combined airflow configurations: parallel-flow followed by counter-flow (*p-f + c-f*) and counter-flow followed by parallel-flow (*c-f + p-f*)

In light of previous results, it seems to be possible to reduce the length of the dryer if we succeed to get a high rate of drying at both the beginning and the end of the tunnel. To this end, air is injected at each end of the dryer with equal flow-rates and the exhaust of gas is located at mid-length of the tunnel: *p-f + c-f* configuration. The opposite configuration (*c-f + p-f*) is also studied (Fig. 8).

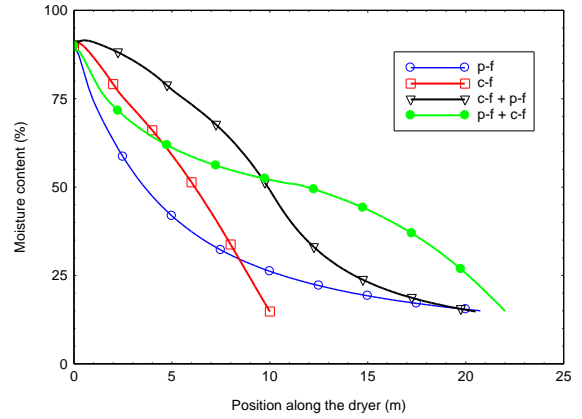


Fig. 9. Simulated evolution of the average *MC* of the bed along the tunnel for simple and combined configurations

Fig. 9 shows that the expected gain is not obtained. The combined configurations do not significantly reduce the length of the dryer, which is against the intuition that led to the study of the combined configurations: the *p-f + c-f* configuration is less efficient than the *c-f + p-f*.

The multiscale model is also useful for studying the impact of an unequal distribution of the air flow-rate within the *c-f* and *p-f* sections or the displacement of the limit between these sections along the dryer. In both cases, the results are similar to the previous: sharing the heat source does not appear to be a promising solution and the *c-f* configuration remains the most efficient.

#### Air recirculation system

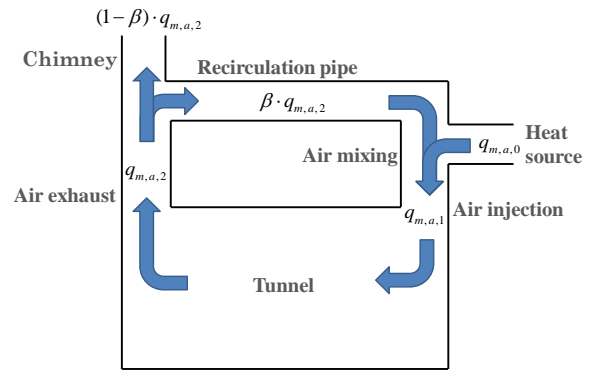


Fig. 10. Schematic diagram of the air recirculation system

A recirculation system can be implemented in order to exploit the full evaporation potential of the air (Fig. 10). The air flow-rate inside the tunnel increase with the recirculation rate  $\beta$  whose value can vary between 0 and 1:

$$q_{m,a,1} = \frac{1}{1-\beta} \cdot q_{m,a,0} \quad (7)$$

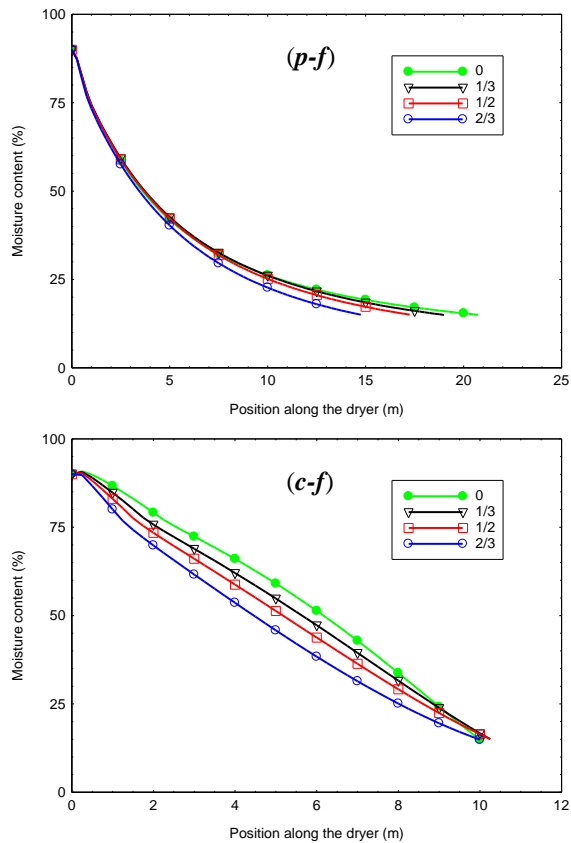


Fig. 11. Influence of the air recirculation rate on the length of the tunnel with *p-f* and *c-f* configurations

Unlike the *c-f* configuration, the air recirculation has a positive effect on the *p-f* configuration (Fig. 11). The increase in recirculation rate significantly reduces the tunnel length. However the tunnel remains longer (14.25 m) than the one with a *c-f* configuration (10 m). Although the air recirculation cannot be used to make the tunnel shorter, it reduces the risk of fire because the temperature of the air injected into the tunnel decreases as the recirculation rate increases (from 120 °C when  $\beta = 0$  to 78.9 °C when  $\beta = 2/3$ ).

#### Optimization of the MC heterogeneity

The *c-f* configuration meets the objective in terms of average MC (15 %) but the heterogeneity remains too high (14 %, Fig. 12). In order to obtain a MC heterogeneity lower than 10 %, we must extend the tunnel by 4.5 m, for a total length of 14.5 m. The average MC of wood is then 5.3 %. An air recirculation rate equal to 2/3 allows the size of the dryer with a *p-f* configuration to be limited to 14.75 m (Fig. 11). In this case, the MC heterogeneity is about 9 %. Both dryers are similar regarding their length but the *c-f* configuration – 14.5 m long – doesn't need an air recirculation system. Thus we choose this design because of its lower investment and operating costs.

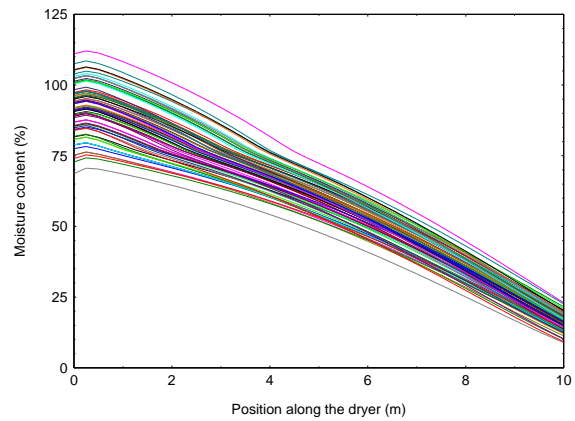


Fig. 12. Unsatisfying decrease of the MC heterogeneity with the *c-f* configuration

Through this example the multiscale model appears to be helpful to design new dryers, to test the relevance of technical solutions and finally to adjust the business plan.

## CONCLUSION

The multiscale model presented in this paper, based on an enhanced Van Meel model at the particle level, is perfectly able to deal with the continuous drying of wood for energy purposes. As main feature, the multiscale structure allows the coupling between the different spatial scales to be accounted for with a huge number of particles (up to several thousands) with different properties. Thus, it is able to account for average fields, standard deviations and local values. Finally, at the drier scale, the calculations of energy efficiency consider the heat flows through the wall and take into account any condensation that may happen at its surface.

Both case studies have demonstrated the potential of this multiscale model as an engineering tool to design or optimize industrial facilities. Indeed it is suitable for a wide range of configurations thanks to its ability to simulate parallel- and counter-flow configuration, several air injection or exhaust points, the air recirculation and the wall thermal insulation. Such a tool allows us reducing investment and operating costs and saving energy while improving the quality of wood drying.

## NOMENCLATURE

$a$	water activity	
$A$	surface area	$m^2$
$A_{lin.spe.}$	linear specific surface area	$m^2 \cdot m^{-1}$
$C$	molar concentration of air	$mol \cdot m^{-3}$
$c_p$	heat capacity	$J \cdot kg^{-1} \cdot K^{-1}$
$H$	heat transfer coefficient	$W \cdot m^{-2} \cdot K^{-1}$
$j_h$	heat flux	$W \cdot m^{-2}$
$j_v$	mass flux	$kg \cdot s^{-1}$
$k_m$	mass transfer coefficient	$m \cdot s^{-1}$
$L_v$	latent heat of vaporization	$J \cdot kg^{-1}$

$M$	molar mass	$\text{kg}\cdot\text{mol}^{-1}$
$m_0$	anhydrous mass of the particle	kg
$P$	pressure	Pa
$q_m$	mass flow-rate	$\text{kg}\cdot\text{s}^{-1}$
$q_v$	volume flow-rate	$\text{m}^3\cdot\text{s}^{-1}$
$RH$	relative humidity	
$T$	temperature	K
$x$	position along the dryer	m
$X$	moisture content	

#### Greek letters

$\beta$	recirculation rate
$\phi$	dimensionless moisture content

#### Subscripts and superscripts

$atm$	atmospheric pressure
$cr$	critical
$db$	dry bulb
$eq$	equilibrium
$in$	inside the dryer
$l$	liquid water
$out$	outside the dryer
$surf$	surface exchange
$v$	water vapor
$vs$	saturation vapor
$\infty$	air-flow

#### REFERENCES

- European Commission. Innovating for sustainable growth: A bioeconomy for Europe. Communication to the European Parliament, the Council, the European Economic and Social Committee and the Committee of the Regions Brussels, Belgium, February 13, 2012.
- Damartzis, T.; Zabaniotou, A. Thermochemical conversion of biomass to second generation biofuels through integrated process design - A review. *Renewable and Sustainable Energy Reviews* **2011**, 15 (1), 366–378.
- Perré, P. Multiscale aspects of heat and mass transfer during drying. *Transport in Porous Media* **2007**, 66 (1-2), 59–76.
- Perré, P.; Remond, R., A Dual scale computational model of kiln wood drying including single board and stack level simulation. *Drying Technology* **2006**, 4 (1-6), 1069–1074.
- Patankar, S.V. Numerical heat transfer and fluid flow; McGraw-Hill Book Company: New York, 1980.
- Perré, P.; Degiovanni, A. Simulation par volumes finis des transferts couplés en milieux poreux anisotropes: Séchage du bois à basse et à haute température. *International Journal of Heat and Mass Transfer* **1990**, 33 (11), 2463–2478.
- Prat, M. 2D modelling of drying of porous media: influence of edge effects at the interface. *Drying Technology* **1991**, 9 (5), 1181–1208.
- Turner, I.W. A two-dimensional orthotropic model for simulating wood drying processes. *Applied Mathematical Modelling* **1996**, 20 (1), 60–81.
- Chen, X.D. A discussion on a generalized correlation for drying rate modeling. *Drying Technology* **2005**, 23 (3), 415–426.
- Sander, A. Thin layer drying of porous materials: Selection of the appropriate model and relationships between thin-layer models parameters. *Chemical Engineering and Processing* **2007**, 46, 1324–1331.
- Van Meel, D.A. Adiabatic convection batch drying with recirculation of air. *Chemical Engineering Science* **1958**, 9, 36–44.
- Saastamoinen, J.; Impola, R. Drying of biomass particles in fixed and moving beds. *Drying Technology* **1997**, 15 (6-8), 1919–1929.
- Colin, J. Séchage en continu du bois énergie comme moyen de préconditionnement en vue de sa conversion thermo-chimique : approches expérimentale et numérique; PhD. Thesis, AgroParisTech, Paris, France, 2011.
- Perré, P.; Turner, I.W. A 3-D version of *TransPore*: a comprehensive heat and mass transfer computational model for simulating the drying of porous media. *International Journal of Heat and Mass Transfer* **1999**, 42 (24), 4501–4521.